

Evolving *Hox* Activity Profiles Govern Diversity in Locomotor Systems

Heekyung Jung,¹ Esteban O. Mazzoni,² Natalia Soshnikova,^{3,4} Olivia Hanley,¹ Byrappa Venkatesh,^{5,6} Denis Duboule,^{3,7} and Jeremy S. Dasen^{1,*}

¹Howard Hughes Medical Institute, NYU Neuroscience Institute, Department of Neuroscience and Physiology, New York University School of Medicine, New York, NY 10016, USA

²Department of Biology, New York University, New York, NY 10003, USA

³Department of Genetics and Evolution, University of Geneva, Sciences III, Quai Ernest-Ansermet 30, 1211 Geneva 4, Switzerland

⁴Institute of Molecular Biology, Ackermannweg 4, 55128 Mainz, Germany

⁵Comparative Genomics Laboratory, Institute of Molecular and Cell Biology, A*STAR, Biopolis, Singapore 138673, Singapore

⁶Department of Paediatrics, Yong Loo Lin School of Medicine, National University of Singapore, Singapore 119228, Singapore

⁷School of Life Sciences, Ecole Polytechnique Fédérale, 1015 Lausanne, Switzerland

*Correspondence: jeremy.dasen@nyumc.org

<http://dx.doi.org/10.1016/j.devcel.2014.03.008>

SUMMARY

The emergence of limb-driven locomotor behaviors was a key event in the evolution of vertebrates and fostered the transition from aquatic to terrestrial life. We show that the generation of limb-projecting lateral motor column (LMC) neurons in mice relies on a transcriptional autoregulatory module initiated via transient activity of multiple genes within the *HoxA* and *HoxC* clusters. Repression of this module at thoracic levels restricts expression of LMC determinants, thus dictating LMC position relative to the limbs. This suppression is mediated by a key regulatory domain that is specifically found in the *Hoxc9* proteins of appendage-bearing vertebrates. The profile of *Hoxc9* expression inversely correlates with LMC position in land vertebrates and likely accounts for the absence of LMC neurons in limbless species such as snakes. Thus, modulation of both *Hoxc9* protein function and *Hoxc9* gene expression likely contributed to evolutionary transitions between undulatory and ambulatory motor circuit connectivity programs.

INTRODUCTION

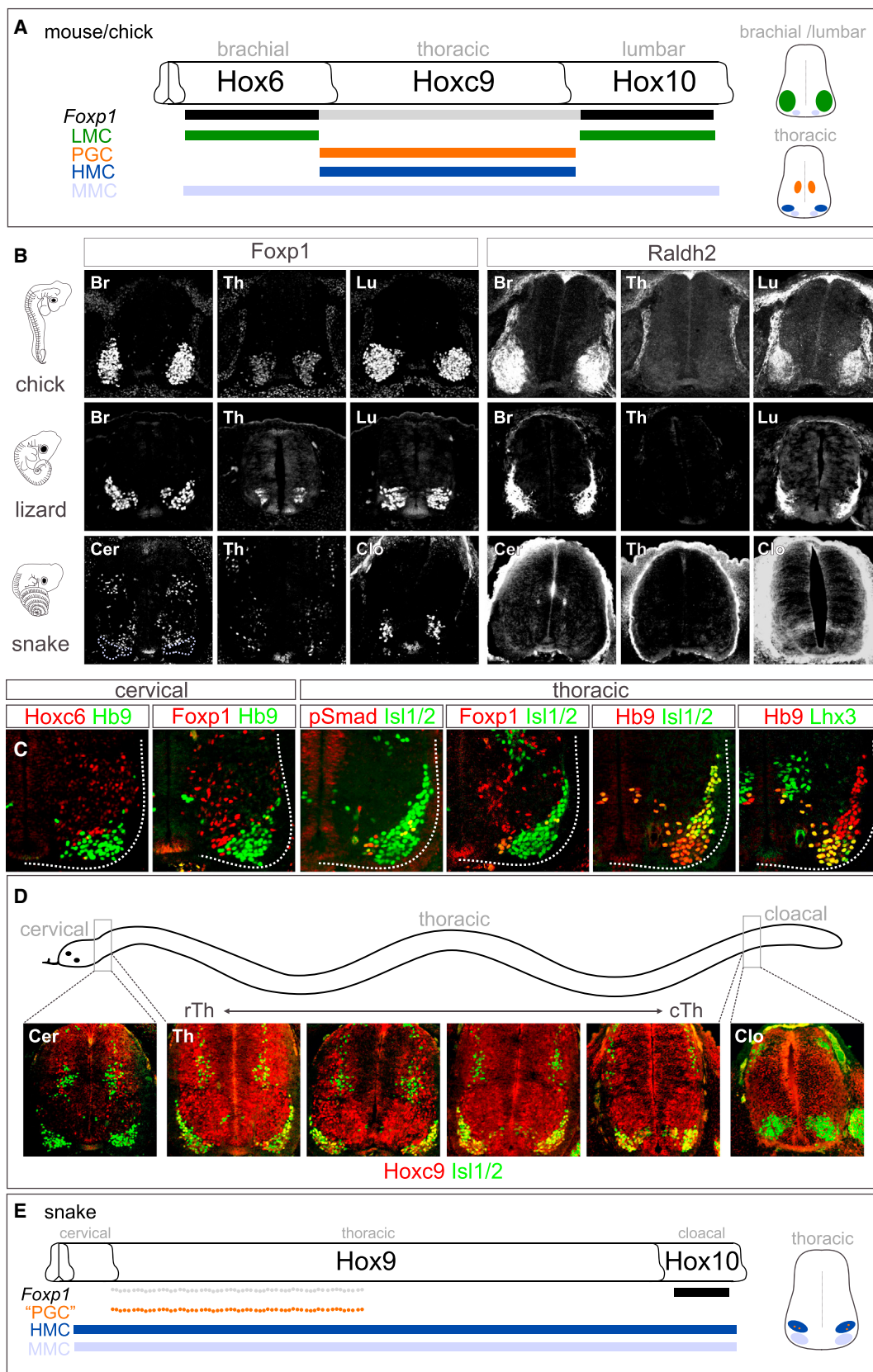
Locomotion is a basic behavior exhibited by virtually all animals. Although species display a wide variety of motor capabilities, land- and water-based locomotion typically employs spinal neural networks whose outputs can be classified as being either ambulatory or undulatory. Undulatory motor behaviors, driven by sinusoidal waves of muscle contraction along the body axis, are observed in a large number of vertebrate and invertebrate species including anguilliform fish, snakes, worms, and insect larvae. Ambulatory behaviors, such as walking, are prominent in tetrapod vertebrates and require the coordinate activation of limb muscle groups by spinal motor neurons. The appearance of a limb-innervation program was a significant

step in expanding the repertoire of motor functions in vertebrates, allowing for a diverse array of behavioral innovations extending beyond locomotion, as exemplified by the range of articulations that can be performed by the human hand.

All motor behaviors rely on the selective innervation of muscles by motor neurons (MNs) residing in the brainstem and spinal cord. The basic program for muscle innervation is conserved across many species and determines features common to all MNs, such as the trajectory of axons toward muscle and the establishment of neuromuscular synapses (Thor and Thomas, 2002; Tripodi and Arber, 2012). Although both vertebrates and invertebrates are capable of walking, the pathway leading to limb innervation is thought to have originated independently in the vertebrate lineage (Murakami and Tanaka, 2011). Vertebrates bearing paired appendages (i.e., fins or limbs) evolved from marine species that lacked appendages and displayed undulatory-type motor behaviors. This locomotor strategy is present in modern representatives of basal chordate lineages including cephalochordates (e.g., amphioxus) and cyclostomes (e.g., lamprey and hagfish) (Grillner and Jessell, 2009). How spinal neuronal circuits evolved to implement limb-based motor strategies remains poorly understood.

The foundation of tetrapod limb-innervation programs emerged in species that used fins to balance and modulate axial muscle-driven swimming behaviors. Studies in ray-finned fish suggest that this program originated through adaptive changes in hindbrain-derived MNs that were initially involved in head bending (Ma et al., 2010). Aspects of the tetrapod limb-innervation program, such as expression of the *retinaldehyde dehydrogenase 2* (*Raldh2*) gene by limb-level MNs, are also present in pectoral MNs of zebrafish embryos (Begemann et al., 2001). Moreover, certain modern and ancient fish species appear to have utilized pectoral appendages for transient excursions on land (Daeschler et al., 2006; Kawano and Blob, 2013), suggesting that the invasion of terrestrial environments by vertebrates was mediated by adaptive changes within forelimb-level locomotor circuits.

In quadrupeds, forelimb and hindlimb muscles are innervated by a column of MNs spanning four to six segments generated in registry with the developing limbs (Landmesser, 2001). Although they arise at distinct levels, brachial and lumbar lateral motor



(legend on next page)

column (LMC) neurons share identical early features. Both populations are defined by expression of the *Foxp1* and *Raldh2* genes, and exhibit similar codes of LIM homeodomain (HD) protein expression (Dasen and Jessell, 2009; Sockanathan and Jessell, 1998; Tsuchida et al., 1994). A key step in LMC specification in mice is the activation of the *Foxp1* gene, encoding a transcription factor required for LMC subtype diversification, and the selection of limb muscles (Dasen et al., 2008; Rousoo et al., 2008). Initiation of the *Foxp1* → *Raldh2* → LIM HD pathway at limb levels is dictated by Hox proteins expressed by MNs at specific rostrocaudal coordinates. Hox6 and Hox10 proteins contribute to the positioning of brachial and lumbar LMC neurons, respectively, whereas Hoxc9 defines intervening thoracic MN populations, including preganglionic and hypaxial motor column (PGC and HMC) neurons (Figure 1A) (Jung et al., 2010). An additional network of ~20 Hox proteins acts within these columnar groupings to specify the identity of MN pools targeting individual muscles (Dasen et al., 2005). Given the critical roles of Hox genes in tetrapod MN specification, it is plausible that they contributed to the appearance of limb-based motor networks, as well as the variations in MN organization observed among vertebrate species (Fetcho, 1992).

We reasoned that insights into the evolution of spinal circuits could emerge by analyzing Hox profiles in species that display distinct motor behaviors and by assessing the activities of Hox proteins derived from more “primitive” vertebrate species. We show here that LMC neurons are specified through induction of the *Foxp1* gene by transient, and somewhat generic, Hox activity. This program is maintained at limb levels through positive *Foxp1* autoregulation, whereas LMC position relative to limbs is defined through Hoxc9-mediated suppression of *Foxp1* at nonlimb levels. This regulatory strategy appears to have emerged early in the development of paired appendages. These findings suggest that modulation in the spatiotemporal profiles and activities of Hox proteins can facilitate nervous system adaptations.

RESULTS

Hox Genes and the Diversity of Vertebrate MN Columnar Organization

To explore the relationship between Hox gene profiles and MN organization in vertebrates, we compared MN columnar subtypes in three representative species of appendage-bearing tetrapod classes: mammals (mice), birds (chicks), and reptiles

(whiptail lizards, *Aspidoscelis uniparens*). We also analyzed MN organization in two species of snake (corn snake, *Pantherophis guttatus*; African house snake, *Lamprophis fuliginosus*), which lack the limb appendages targeted by LMC neurons. We examined the profile of markers for columnar subtypes dependent on Hox genes: LMC neurons at limb levels, PGC and HMC neurons at thoracic levels, and Hox-independent medial motor column (MMC) neurons (Figure 1A). In lizard embryos, LMC neurons were present, as limb-level MNs settled in a ventrolateral position and expressed high levels of *Foxp1* and *Raldh2* (Figure 1B). At thoracic levels, a subset of MNs migrated dorsally, expressed low levels of *Foxp1*, and was labeled by phospho (p)Smad1/5/8, indicative of a PGC identity (Figure 1B; Figure S1A available online). Whereas HMC (*Hb9*⁺, *Isl1/2*⁺) neurons were predominantly found at thoracic levels, axial projecting MMC neurons (*Hb9*⁺, *Lhx3*⁺) were present at all rostrocaudal levels (Figures S1B and S1C). These analyses reveal that the basic program for columnar organization is largely conserved in tetrapod species.

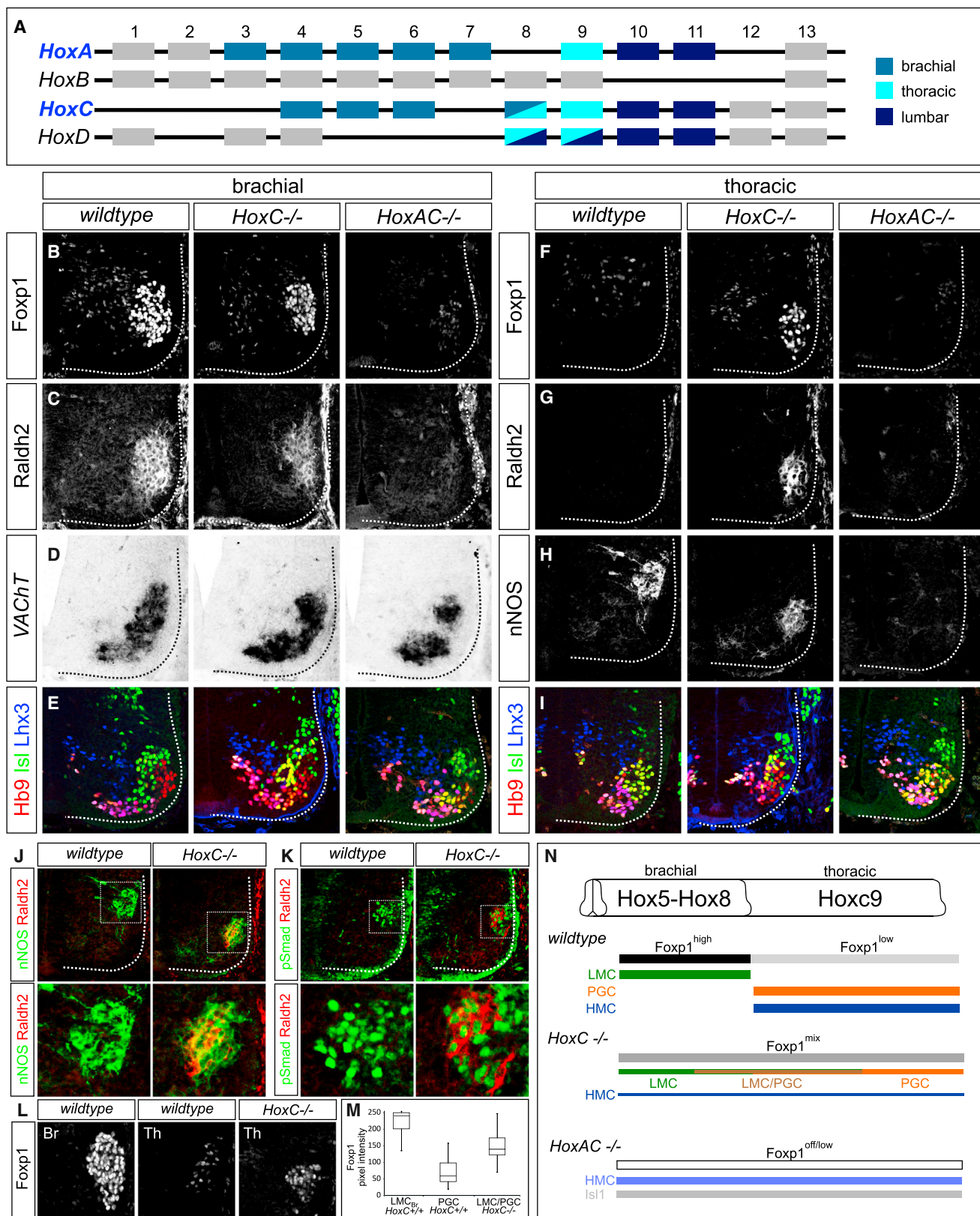
In contrast, snake embryos lacked discernible LMC populations, as *Foxp1*^{high}, *Raldh2*⁺ MNs were not detected at any level (Figures 1B and 1C). Instead, snakes displayed an extended thoracic columnar organization, as MMC and HMC neurons were found throughout the spinal cord (Figure 1C; Figures S1B and S1C). PGC-like neurons (pSmad1/5/8⁺, *Foxp1*^{low}, *Hb9*⁻, *Isl1/2*⁺) were present at thoracic levels but were scattered within the ventral horn, suggesting an alternative organization for this population (Figures 1B and 1C; Figure S1A). At cloacal levels, a ventrolateral cluster of *Foxp1*⁺ MNs was observed in a region that occupied the same segments as the genital tubercles (Figure 1B). These MNs expressed the lumbar determinant *Hoxd10* but did not express *Raldh2* or display the LIM HD profile characteristic of LMC neurons (Figure 1B; Figures S1F and S1G).

Profiles of Hox expression paralleled the marked differences in columnar organization observed between snakes and other tetrapods. Lizards displayed a pattern of Hox expression in MNs similar to chicks and mice (Figures S1D–S1F). In contrast, Hoxc6 was not expressed by MNs in snakes, and most of ~200 thoracic segments expressed Hoxc9, indicating a broad rostrocaudal extension in its expression domain (Figures 1C and 1D; Figures S1D and S1E). These observations indicate that the lack of a forelimb LMC program, in conjunction with an increase in the number of thoracic segments, is associated with an expanded domain of Hoxc9 (Figure 1E).

Figure 1. Analysis of MN Columnar Organization and Hox Gene Profiles in Vertebrates

- (A) Summary of MN columnar subtypes and their key determinants in mouse and chick spinal cord. Hox-dependent LMC and PGC neurons are specified through high and low levels of *Foxp1*, respectively. Right: schematics of transverse sections showing MN position.
- (B) Comparison of *Foxp1* and *Raldh2* patterns in chick, lizard, and snake embryos. In snake, *Foxp1*^{high}, *Raldh2*⁺ MNs were not found at any spinal level. Dotted areas indicate the positions of MNs. Chick embryos are shown at HH stage 27, lizard embryos at 10–11 dpo (days postoviposition), and snake embryos at 8–9 and 9–10 dpo. Br, brachial; Th, thoracic; Lu, lumbar; Cer, cervical; Clo, cloacal.
- (C) MN columnar organization in snake embryos at 9–10 and 10–11 dpo. MNs were labeled by *Hb9* or *Isl1/2* in each panel. At cervical levels, Hoxc6 and *Foxp1* are restricted to dorsal interneuron populations. At thoracic levels, PGC-like MNs (pSmad1/5/8⁺, *Foxp1*^{low}) were detected in a scattered distribution, and HMC (*Hb9*⁺, *Isl1/2*⁺) neurons and MMC (*Hb9*⁺, *Lhx3*⁺) neurons were present. Dotted lines outline the ventral quadrant of the spinal cord.
- (D) Expansion of Hoxc9 expression throughout thoracic levels in snake. Hoxc9 expression was observed in cervical interneurons and thoracic MNs, but was absent from cloacal levels at 9–10 dpo. cTh, caudal thoracic; rTh, rostral thoracic.
- (E) Summary of Hox patterns and MN columnar organization in snake embryos. The scattered distribution of PGC-like MNs likely reflects cross-repressive interactions between *Foxp1* and *Hb9* within Hoxc9⁺ MNs (Dasen et al., 2008).

See also Figure S1.

**Figure 2. Loss of MN Columnar Identities in Hox Cluster Mutants**

(A) Summary of Hox expression profiles in MNs of limb-bearing tetrapods. Hox genes expressed by MNs at different levels are color coded.
 (B–I) Defects in MN columnar specification in *HoxC* and *HoxA/HoxC* cluster mutants at brachial (B–E) and thoracic (F–I) levels at e11.5.

(legend continued on next page)

Erosion of Motor Neuron Columnar Identities in Hox Cluster Mutants

The absence of LMC neurons in snake embryos is consistent with the idea that *Hoxc9* represses limb-innervation programs. This observation is also in agreement with the finding that in *Hoxc9* mutant mice all thoracic MNs are transformed to a brachial LMC identity (Jung et al., 2010). To understand how *Hoxc9* mediates LMC suppression, we first sought to resolve the Hox-dependent mechanisms through which limb-innervating MNs are normally specified. Misexpression studies in chick indicate that *Hox5–Hox8* paralogs can impose an LMC identity onto thoracic MNs, suggesting that multiple *Hox* genes contribute to LMC fate (Lacombe et al., 2013). To definitively assess *Hox* function in MN columnar specification, we determined the consequences of eliminating several *Hox* genes in mice. Because the majority of *Hox* genes expressed by brachial and thoracic MNs are concentrated within the *HoxA* and *HoxC* gene clusters (Figure 2A) (Dasen et al., 2005), we analyzed MN specification in *HoxA* and *HoxC* gene cluster mutants at embryonic day (e)12.5 (Kmita et al., 2005; Suemori and Noguchi, 2000).

In the absence of the *HoxC* cluster, the number of forelimb LMC neurons was reduced by ~40%, assessed by the number of *Foxp1^{high}*, *Raldh2⁺* MNs (Figures 2B and 2C; Figure S2A). Total MN number was grossly unchanged in *HoxC* mutants, and the specification of Hox-independent, axially projecting MMC neurons was unaffected (Figures 2D, 2E, and 2I). Hindlimb-innervating LMC neurons developed normally, consistent with a prominent role for *HoxD* genes in their specification (Figure S2B) (Shah et al., 2004; Wu et al., 2008). In contrast, brachial MN pools, defined by expression of the transcription factors *Pea3* and *Scip*, were markedly depleted in *HoxC* cluster mutants (Figure S2C), consistent with a requirement for *Hoxc6* and *Hoxc8* in these subtypes (Lacombe et al., 2013; Vermot et al., 2005).

Genes in the *HoxA* cluster have been implicated in LMC specification (Lacombe et al., 2013), and could be responsible for its perseverance in *HoxC* mutants. In support of this idea, we found that there is an elevation in *HoxA* expression in *HoxC* mutants (Figures S2D and S2E). We therefore analyzed mice mutant for both the *HoxA* and *HoxC* clusters. Analysis of *Foxp1* and *Raldh2* expression at e12.5 in *HoxA/HoxC* mutants revealed a marked loss of brachial LMC neurons (Figures 2B and 2C). Low levels of *Foxp1* were detected in *HoxA/HoxC* mutants, although this was apparently insufficient to promote critical aspects of LMC identity such as *Raldh2* expression (Figure S2F). Thoracic PGC neurons were also absent in *HoxA/HoxC* mutants, consistent

with a requirement for *Hoxc9* and *Hoxa9* (Figure 2H) (Dasen et al., 2003). These observations indicate that only through combined deletion of the *HoxA* and *HoxC* clusters is brachial LMC identity effectively erased from MNs.

Hybrid Motor Neuron Columnar Identities in HoxC Cluster Mutants

In contrast to the multiple *Hox* inputs controlling MN identity at brachial levels, thoracic fates are determined by the single *Hoxc9* gene, which represses brachial *Hox4–Hox8* genes at thoracic levels and sets low *Foxp1* levels in PGC neurons (Jung et al., 2010). In *HoxC* mutants, we expected that ectopic LMC neurons would be generated throughout thoracic levels, due to derepression of *HoxA* genes. Surprisingly, we detected markers of both LMC and PGC neurons at thoracic levels in *HoxC* mutants (Figures 2F–2H). These MNs occupied the same ventrolateral position, suggesting that some acquired a “hybrid” columnar identity. Consistent with this idea, *Raldh2⁺/pSmad⁺* and *Raldh2⁺/neuronal nitric oxide synthase (nNOS)⁺* neurons were observed in *HoxC* mutants (Figures 2J and 2K). The extent of this phenotype varied along the rostrocaudal axis, with MNs coexpressing LMC and PGC determinants extending from caudal brachial to rostral thoracic levels, likely reflecting differential compensation by *HoxA* genes.

Foxp1 has been suggested to act as a dose-dependent determinant of LMC and PGC identities, and *Foxp1* overexpression can convert PGC and HMC neurons to an LMC fate (Dasen et al., 2008). To understand why hybrid LMC/PGC neurons were generated, we analyzed *Foxp1* levels in *HoxC* mutants. We observed *Foxp1* levels that were intermediate to that of wild-type brachial LMC and thoracic PGC neurons (Figures 2L and 2M). Thus, attenuation of the normal Hox inputs in MNs generates cells with inappropriate *Foxp1* levels and hybrid molecular identities. Collectively, these results indicate that a primary function of *Hox* genes in tetrapod MNs is to set *Foxp1* levels, with multiple Hox proteins promoting high levels in LMC neurons at limb levels, whereas *Hoxc9* dampens *Foxp1* at thoracic levels (Figure 2N).

Conservation and Variation of Hox9 Paralog Activities in Motor Neurons

Analysis of *Hox* cluster mutant animals indicates that programming of LMC fate involves an activity shared by many *Hox* genes, whereas *Hoxc9* has a selective function in preventing thoracic MNs from acquiring an LMC fate. These findings support the

(B and C) LMC neurons (*Foxp1^{high}*, *Raldh2⁺*) were reduced in *HoxC* mutants and lost in *HoxA/HoxC* mutants.

(D) The total number of brachial MNs remained grossly unchanged in *HoxC* mutants, but was reduced by ~30% in *HoxA/HoxC* mutants, similar to the loss observed in *Foxp1* mutants, in which LMC specification is similarly affected (Dasen et al., 2008).

(E) MNs with an HMC molecular profile (*Hb9⁺*, *Isl1/2⁺*, *Lhx3⁻*) were increased in both *HoxC* and *HoxA/HoxC* mutants.

(F–H) Both LMC and PGC markers were detected in *HoxC* mutants, but were absent in *HoxA/HoxC* mutants.

(I) Analysis of MN molecular profiles (*Hb9*, *Isl1/2*, *Lhx3*) revealed that total thoracic MN numbers were similar between wild-type and *HoxC* and *HoxA/HoxC* mutants. MMC neurons (*Hb9⁺*, *Isl1/2^{low}*, *Lhx3⁺*) were grossly unaffected in both mutants.

(J and K) Analysis of LMC/PGC hybrid MNs in *HoxC* mutants at thoracic levels. *Raldh2⁺* MNs coexpress the PGC markers nNOS and pSmad1/5/8. Bottom: magnified images of boxed areas in upper panels.

(L and M) Comparison of *Foxp1* expression levels at brachial and thoracic in wild-type and thoracic spinal cord in *HoxC* mutants.

(M) Lower and upper bars in box plots indicate minimum and maximum nuclear pixel intensities, respectively.

(N) Summary of altered MN columnar organization in *HoxC* and *HoxA/HoxC* cluster mutants. In *HoxA/HoxC* mutants a population of *Isl1⁺*; *Hb9⁻* MNs is also present.

See also Figure S2.

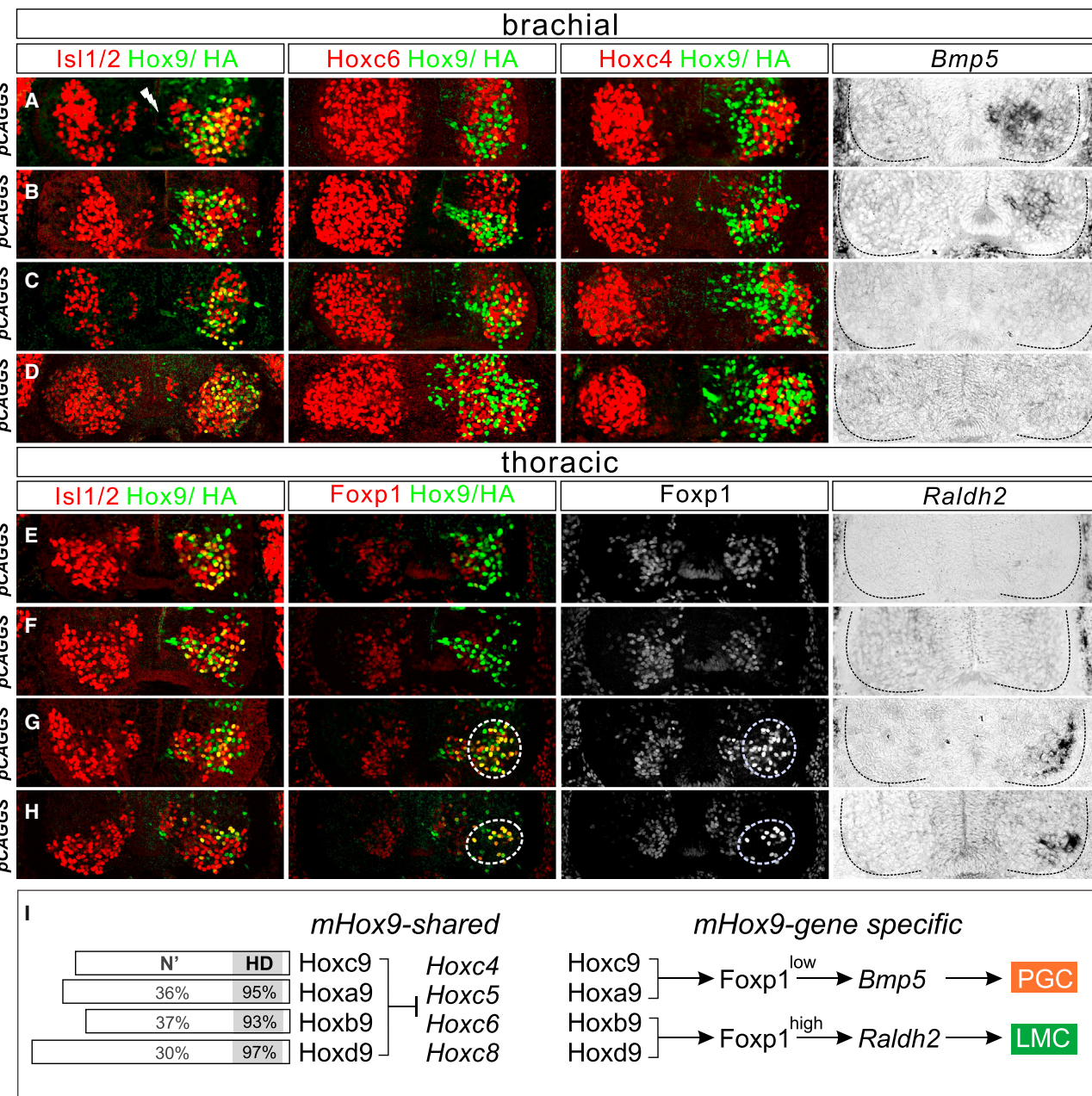


Figure 3. Shared and Distinct Activities of Hox9 Proteins in MNs

Effects of murine *Hox9* gene misexpression via *in ovo* electroporation at brachial (A–D) and thoracic (E–H) levels. To determine whether Hox9 proteins were expressed in MNs, *Isl1/2* and *Hox9/HA* co-staining is shown (left).

(A–D) All four m*Hox9* paralogs cell autonomously repressed *Hoxc6* and *Hoxc4* at brachial levels. *Hoxa9* and *Hoxc9* misexpression lowered *Foxp1* levels (see Figures S3B and S3C) and induced ectopic PGC (*Bmp5*⁺) neurons at brachial levels. The electroporated side of the spinal cord is indicated by a white bolt.

(E–H) Expression of *Hoxb9* and *Hoxd9* at thoracic levels induced ectopic LMC neurons as assessed by high levels of *Foxp1* and *Raldh2*, and these MNs migrated to a ventrolateral position. Unless otherwise indicated, dotted circles outline ectopic LMC neurons.

(I) Summary of shared and gene-specific functions of the four m*Hox9* paralogs in MNs. Schematics (left) indicate the percentage of amino acids at the N terminus (N') and homeodomain conserved between the indicated paralog and m*Hoxc9*.

See also Figure S3.

idea that the *Hoxc9* gene has a central role in determining MN columnar organization in vertebrates. In principle, the restricted actions of *Hoxc9* could reflect selective binding to specific MN gene targets, or target recognition-independent activities medi-

ated by regions outside the homeodomain. To examine this question *in vivo*, we first determined whether the activities of *Hoxc9* are displayed by additional *Hox9* paralogs (*Hoxa9*, *Hoxb9*, *Hoxd9*) (Figure 3). All murine (m)*Hox9* proteins share

highly conserved homeodomains but display limited homology outside this region (Figure 3I; Figure S3A). To test the specificity of *Hoxc9* paralog activity, we compared their function in relation to two activities of *Hoxc9*: (1) a repressive activity toward *Hox4–Hox8* genes, and (2) the ability to attenuate *Foxp1* expression levels in PGC neurons.

We used *in ovo* chick electroporation to misexpress murine *Hoxc9* genes at brachial and thoracic levels and determined their effects on *Hox* expression and columnar differentiation. Each of the four *mHoxc9* paralogs repressed brachial *Hox* genes, as assessed by their ability to cell autonomously extinguish *Hoxc4* and *Hoxc6* expression (Figures 3A–3D). Consistent with previous studies, *Hoxa9* activity was identical to *Hoxc9* and promoted PGC fates (*Bmp5⁺*, *Foxp1^{low}*) at brachial levels (Figures 3A, 3B, 3E, and 3F; Figures S3B and S3C) (Dasen et al., 2003; Jung et al., 2010). In contrast, *Hoxb9* and *Hoxd9* failed to induce PGC identity or suppress LMC specification at brachial levels (Figures 3C and 3D and data not shown). Remarkably, MNs expressing *Hoxb9* or *Hoxd9* at thoracic levels migrated to a ventrolateral position and induced high levels of *Foxp1* and *Raldh2*, indicative of a conversion to an LMC fate (Figures 3G and 3H). After *Hoxb9/d9* misexpression, *Hoxc9* expression was retained, indicating that LMC induction is not simply due to the extinction of endogenous *Hoxc9* (Figures S3D and S3E). These data indicate that the repressive activity toward brachial *Hox* genes is conserved in all murine *Hoxc9* paralogs, whereas the promotion of PGC identity and suppression of LMC fate are specific activities of *Hoxa9* and *Hoxc9*, likely reflecting divergence of functional motifs among *Hoxc9* proteins (Figure 3I).

Tetrapod *Hoxc9* Contains a Latent LMC-Promoting Activity

The ability of each *Hoxc9* paralog to repress brachial *Hox* genes indicates that they are capable of regulating the same set of target genes, implying that regions outside the DNA recognition motif are responsible for their *in vivo* specificities. To define functional domains in *Hoxc9*, we generated a series of N-terminal deletion constructs and tested their activities *in vivo*. We first mapped the peptide sequences within the *mHoxc9* protein required for repression of *Hox4–Hox8* genes. This analysis revealed a repression domain positioned between amino acids 73 and 101, as expression of *mHoxc9NΔ101* failed to repress *Hoxc4* and *Hoxc6* at brachial levels, whereas *mHoxc9NΔ72* retained repressive activity (Figures 4A–4F; Figures S4A–S4F).

Alignment of *Hoxc9* protein sequences across the region required for *Hox* repression revealed a domain of sequence homology present in all four *mHoxc9* paralogs and in other vertebrate *Hoxc9* orthologs (Figure 4I; Figure S5A) (Izpísúa-Belmonte et al., 1991). To test functional conservation of this motif, we generated mutant derivatives of *mHoxd9* equivalent to *mHoxc9NΔ72* and *mHoxc9NΔ101* (*mHoxd9NΔ98* and *mHoxd9NΔ132*, respectively) and tested their activities *in vivo*. Consistent with conserved activity, *mHoxd9NΔ132* failed to repress brachial *Hox* genes, whereas *mHoxd9NΔ98* repressed *Hoxc4* and *Hoxc6* (Figures 4G and 4H; Figures S4G and S4H).

We next tested the ability of *Hoxc9* mutant derivatives to promote MN columnar identities. N-terminal deletions that retain *Hox* repressive functions exhibited normal activity; *mHoxc9NΔ72* generated ectopic PGC neurons at brachial levels (Figure S4C)

and *mHoxd9NΔ98* promoted LMC fates at thoracic levels (Figure 4G). In contrast, *mHoxc9NΔ101* and *mHoxc9NΔ137* failed to induce ectopic PGC neurons at brachial levels (Figures S4D and S4E). Remarkably, both *mHoxc9NΔ101* and *mHoxc9NΔ137* induced LMC identity, as assessed by the presence of ectopic *Foxp1^{high}* and *Raldh2⁺* MNs at thoracic levels (Figures 4D and 4E). In contrast, a large deletion (*mHoxc9NΔ174*), which retains the region required for high-affinity DNA binding, was inactive (Figure 4F; Figure S4F).

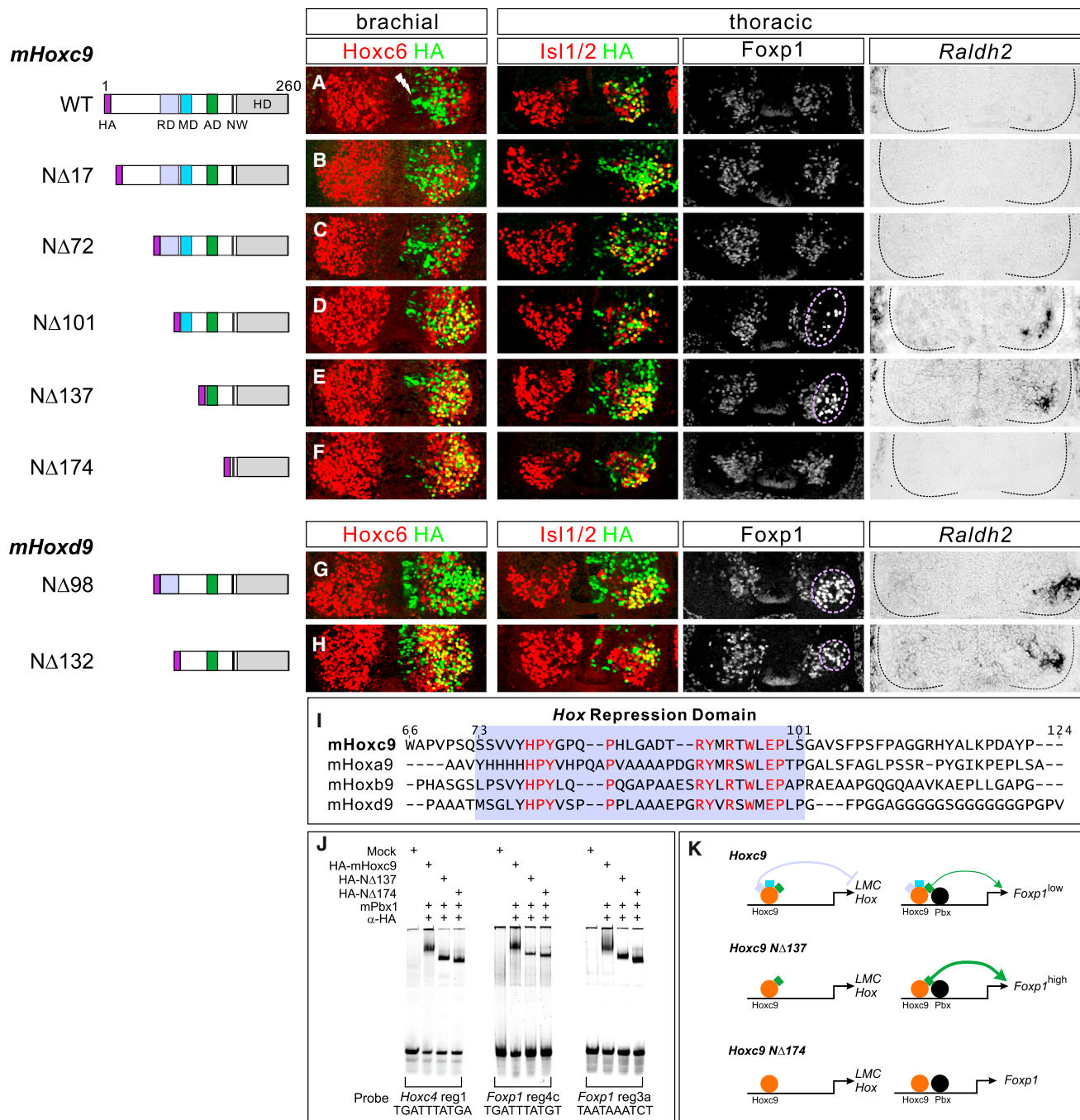
Because the *Hoxc9* mutant derivatives could influence the selectivity of target recognition, we also performed gel mobility shift assays to determine whether DNA binding is preserved. We tested mutant *Hoxc9* proteins on a binding site located within the *HoxC* cluster and two conserved sites within the *Foxp1* gene that are occupied by *Hoxc9* *in vivo* (Figure 4J; see Figure 7A below). We found that both *mHoxc9NΔ137* and *mHoxc9NΔ174* bound to each of these sites in the presence of Pbx cofactors (Figure 4J), indicating that *Hoxc9* DNA binding activity is retained in the absence of its N terminus.

Collectively, these results demonstrate that although *Hoxc9* normally promotes thoracic PGC fates by attenuating *Foxp1* expression, it possesses a dormant LMC-promoting activity that is unleashed after removal of the region containing the repression domain (Figure 4K).

The Emergence of *Hoxc9* Activities in Chordates

These observations raise the questions of how the specific activities of *Hoxc9* emerged in chordates and what accounts for the differences in the columnar identities promoted by murine *Hoxc9* paralogs. We considered the possibility that *Hoxc9* acquired an LMC-suppressing/PGC-promoting activity concomitant with the appearance of paired appendages. We therefore compared *Hoxc9* amino acid sequences based on two criteria: (1) the presence or absence of paired appendages, and (2) the ability of *Hoxc9* proteins to promote either PGC or LMC fate *in vivo*. Inspection of sequences C-terminal to the core *Hox* repression domain revealed an additional motif present in *Hoxc9* proteins that suppress LMC identity and in *Hoxc9* proteins from species bearing paired appendages (Figures 5A and 5B). In contrast, this motif is either absent, degenerated, or shifted from its normal position in murine *Hoxc9* genes that promote LMC fate and in limbless chordates and cephalochordates (Figures 5A and 5B; Figure S5A). We refer to this motif as the *Foxp1* modulatory domain (MD) to distinguish it from the repressive domain (RD) necessary to extinguish brachial *Hox* genes.

To test whether the presence of the MD mediates LMC suppression *in vivo*, we tested the activities of several *Hoxc9* genes by *in ovo* chick electroporation. We isolated *Hoxc9* genes from the limbless species amphioxus and lamprey as well as the pectoral fin-bearing species coelacanth, pufferfish, zebrafish, and elephant shark. Each species carried the core *Hox RD* (Figure 5A; Figure S5A), and was capable of repressing *Hoxc4* and *Hoxc6* at brachial levels (Figures 5C–5H; Figures S5B and S5D). *Hoxc9* genes from appendage-bearing vertebrates functioned as PGC determinants and suppressed LMC specification at brachial levels (Figures 5C–5G; Figure S5B). In contrast, the single *Hoxc9* gene from amphioxus (*Bfl-Hoxc9*), which lacks the MD, acted as an LMC determinant, as it induced *Foxp1^{high}* and *Raldh2* at thoracic levels (Figure 5H; Figure S5B). Two of the *Hoxc9* genes

**Figure 4. Hoxc9 Contains a Latent LMC-Promoting Activity**

Identification of functional domains within Hox9 proteins. Schematics of mHoxc9/mHoxd9 truncations are shown (left). Mutant constructs were HA tagged at the N terminus. RD, Hox repression domain; MD, Foxp1 modulatory domain; AD, Foxp1 activation domain; NW, conserved Pbx interaction motif.

(A–C) mHoxc9NΔ17 and mHoxc9NΔ72 retained normal repressive activity toward Hoxc6 at brachial levels.

(D and E) mHoxc9NΔ101 and mHoxc9NΔ137 failed to repress Hoxc6 at brachial levels and induced ectopic LMC neurons (Foxp1^{high}, Raldh2⁺) at thoracic levels. Ectopic LMC induction was not due to derepression of anterior Hox genes (see Figures S4I and S4J).

(F) mHoxc9NΔ174 lost both Hox repressive and columnar promoting activities (see also Figure S4F).

(G and H) mHoxd9NΔ132 failed to repress Hoxc6 at brachial levels, whereas mHoxd9NΔ98 retained repressive activity. Both constructs displayed LMC-promoting activity at thoracic levels.

(I) Sequence alignment of mHox9 paralogs revealed a conserved region between residues N73 and N101 in mHoxc9 (boxed in purple). Highly conserved residues are shown in red.

(J) Binding of Hoxc9 mutant derivatives to elements in *Hoxc4* and *Foxp1* loci indicated that N-terminal deletions did not affect DNA binding activity.

(legend continued on next page)

from lamprey acted as weak repressors of *Foxp1*, likely due to the presence of an MD-like region in these proteins (Figures S5A, S5D, and S5E).

Among vertebrate Hox9 homologs, the sequence of zebrafish Hoxd9 (*DrHoxd9a*) was distinct from that of mouse. *DrHoxd9a* contains the conserved MD in proximity to the *Hox* RD, and promoted PGC fate at brachial levels (Figures 5A and 5F). To test whether removal of the MD would convert *DrHoxd9a* to an LMC determinant, we generated an N-terminal truncation in *DrHoxd9a* (NΔ140) equivalent to mHoxc9NΔ137, which lacks the MD. Consistent with a requirement for this motif to suppress LMC specification, *DrHoxd9a*NΔ140 induced *Foxp1*^{high} and *Raldh2* at thoracic levels (Figure 5I).

To further assess whether the modular domain contributes to the ability of mHoxc9 to suppress *Foxp1*, we generated internal deletion constructs lacking the *Hox* RD [mHoxc9NΔ(73–101)], the *Foxp1* MD [mHoxc9NΔ(114–121)], and both the RD and MD [mHoxc9NΔ(73–121)] and tested their activities in vivo. With deletion of either the MD or RD, Hoxc9 derivatives retained LMC-suppressing/PGC-promoting activity, although the RD mutant failed to repress brachial *Hox* genes (Figures 5J and 5K; Figure S5C). Combined deletion of the RD and MD converted Hoxc9 to an LMC inducer (Figure 5L), suggesting some degree of functional redundancy in these motifs with respect to *Foxp1* regulation. Together, these observations indicate that Hoxc9 relies on specific motifs in its N terminus to repress LMC specification at thoracic levels, and suggest that this activity emerged at the time vertebrates acquired paired appendages.

***Foxp1* Autoregulation Mediates LMC Specification**

To resolve the mechanisms governing the actions of Hoxc9 during MN columnar organization, we focused on understanding how Hoxc9 suppresses activation of LMC determinants. Analysis of the spatial and temporal profiles of Hox proteins and *Foxp1* expression provided some insight into this question. At thoracic levels, Hoxc9 expression is maintained by PGC neurons between e10.5 and e14.5, whereas *Foxp1* is only transiently expressed (Figure 6A). In contrast, in LMC neurons, *Hox* genes are transiently expressed by MNs between e10.5 and e12.5, whereas *Foxp1* expression is sustained at high levels (Figure 6A and data not shown). These observations suggest a model in which LMC identity is promoted through transient expression of Hox proteins in MNs, which activates *Foxp1*. This pattern continues in the absence of Hox input, possibly through *Foxp1* autoregulation. In contrast, the extended expression of Hoxc9 acts to dampen, and eventually silence, *Foxp1* expression in PGC neurons, effectively preventing deployment of the LMC-specific autoregulatory circuit (Figure 6A).

To test these models, we determined whether sustained expression of *Foxp1* in LMC neurons relies on its autoregulation. To analyze *Foxp1* regulation, we generated a transgenic reporter line using a bacterial artificial chromosome (BAC) containing ~195 kb of the 5' *Foxp1* sequence and inserted GFP at the initiating codon (Figure 6B). Analysis of e11.5 *Foxp1*::GFP embryos

revealed robust expression of the reporter in LMC and low levels in PGC neurons, whereas GFP was absent from MMC and HMC neurons, thus recapitulating the endogenous *Foxp1* pattern (Figure 6B and data not shown).

In principle, if *Foxp1* autoregulates in LMC neurons, reporter expression in *Foxp1*::GFP mice would be lost in a *Foxp1* mutant background. Consistent with this idea, GFP expression was markedly depleted from MNs in *Foxp1*::GFP; *Foxp1*^{−/−} mice at e13.5 (Figure 6C). Analysis of GFP between e10.5 and e13.5 in *Foxp1*::GFP; *Foxp1*^{−/−} mice indicated that the reporter was expressed in MNs between e10.5 and e11.5, albeit at lower levels, indicating that *Foxp1* is not needed for its initial activation (Figure 6D; Figure S6). In addition, we introduced the *Foxp1*::GFP BAC reporter line into a *Hoxc9* mutant background and analyzed embryos at e12.5. We observed ectopic GFP expression throughout the thoracic spinal cord (Figure 6E), consistent with the derepression of *Hox5–Hox8* genes and the extension of high *Foxp1* expression in *Hoxc9* mutants. These data indicate that the *Foxp1*::GFP reporter contains *cis* elements necessary for regulation by Hox proteins and that high *Foxp1* transcription relies on autoregulation.

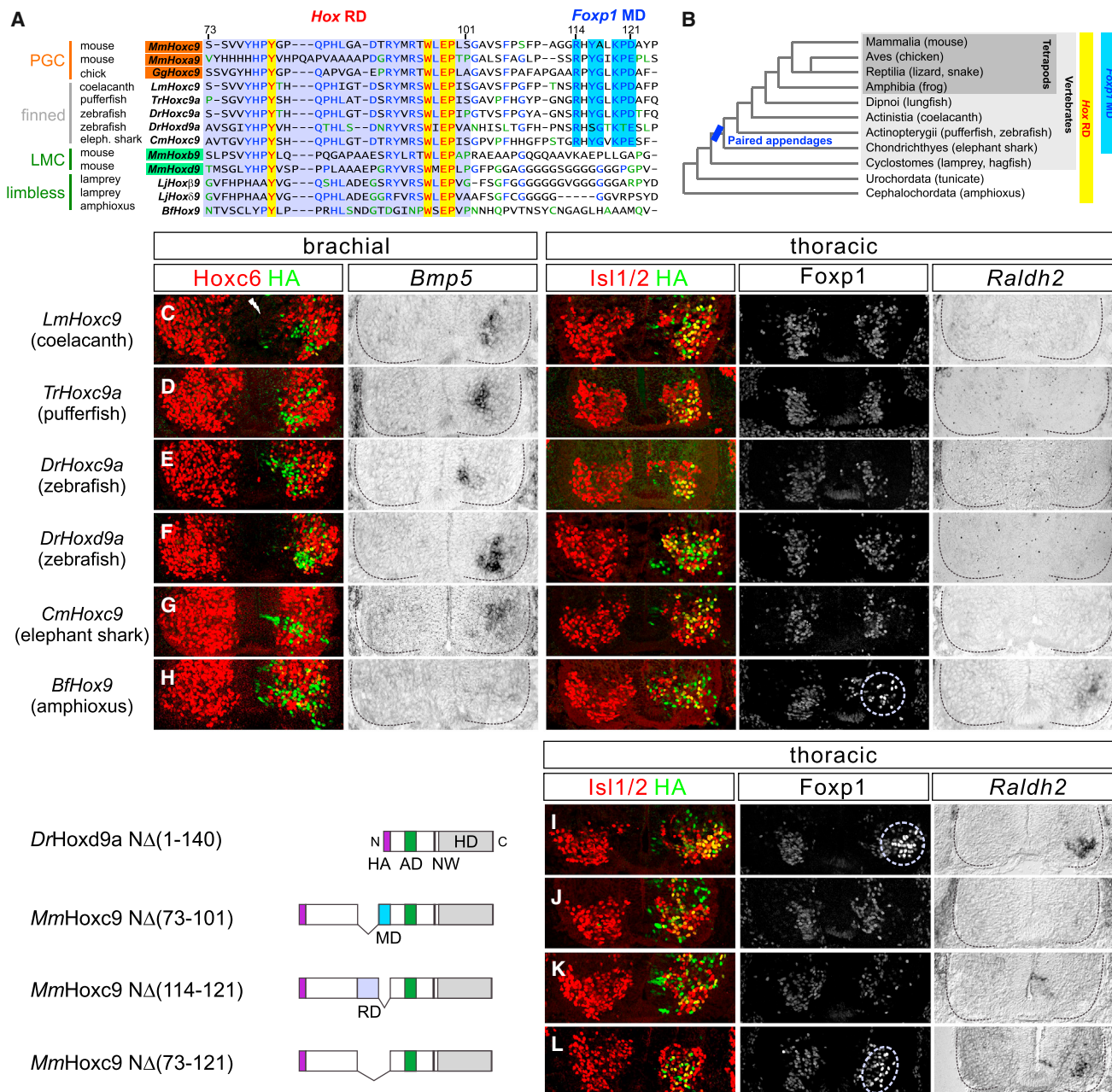
***Foxp1* Responds to Multiple Hox Inputs**

Because *Foxp1* appears to respond to the activities of multiple Hox proteins, we assessed the role of Hox proteins in the direct regulation of *Foxp1*. Analysis of a previous genome-wide characterization of Hoxc9 binding in embryonic stem cell-derived MNs identified two regions within the *Foxp1*::GFP BAC containing potential Hox sites (Figure 7A) (Jung et al., 2010). Alignment of these candidate sites revealed high sequence conservation among vertebrates (Figure S7A). To determine whether these sites are occupied by LMC-promoting Hox proteins at limb levels, we performed chromatin immunoprecipitation assays and found that Hoxc6 binds the same regions in vivo (Figure 7B). In vitro protein analysis of DNA binding revealed that multiple Hox proteins expressed by spinal MNs (Hoxc6, Hoxc8, Hoxc9) are capable of binding to these sites cooperatively with Pbx1 (Figure 7C). In contrast, Hoxb1, which specifies MN subtype identity in the hindbrain (Studer et al., 1996), failed to effectively bind the *Foxp1* sites or affect columnar differentiation when misexpressed in vivo (Figure 7C; Figure S7B). These results indicate that Hox sites in the *Foxp1* gene can be engaged by a variety of Hox proteins expressed by spinal MNs, but are refractory to Hoxb1.

To investigate whether the Hox sites within the *Foxp1*::GFP BAC are functional in vivo, we deleted one or both elements and performed founder analysis at e11.5. Mutation of individual Hox sites in the *Foxp1*::GFP BAC did not alter reporter expression in MNs, suggesting functional redundancy (Figure S7C). After deletion of both sites, expression of GFP was markedly reduced in LMC neurons relative to wild-type *Foxp1*::GFP embryos generated under identical conditions (Figure 7D; Figure S7D). In addition, we detected ectopic GFP expression in HMC neurons at thoracic levels in the mutant construct,

(K) A conserved repression domain (depicted in purple) is required to extinguish anterior *Hox* genes from thoracic levels. A latent activation domain (in green) is unleashed when the *Hox* repression domain is deleted. Models presume the mutant derivatives displace endogenous Hox proteins from the *Foxp1* locus.

See also Figure S4.

**Figure 5. Evolution of Hox9 Function in Chordates**

(A) Alignment of Hox9 proteins from multiple chordate species revealed a conserved motif (boxed in blue) C-terminal to the Hox repression domain present in species with paired appendages. This motif is either absent or shifted C-terminally in other Hox9 proteins (see Figure S5A). *Mm*, *Mus musculus*; *Gg*, *Gallus gallus*; *Lm*, *Latimeria menadoensis*; *Tr*, *Takifugu rubripes*; *Dr*, *Danio rerio*; *Cm*, *Callorhinichthys millii*; *Lj*, *Lethenteron japonicum*; *Bf*, *Branchiostoma floridae*. The Hox repression domain is boxed in purple, and highly conserved amino acids are in yellow.

(B) The presences of the Hox repression domain and Foxp1 modulatory domain are shown in relation to chordate phylogeny.

(C–H) Analysis of Hox9 activities from various chordate species. Hox repressive activity was observed in all Hox9 homologs tested.

(F) Unlike *MmHoxd9*, its ortholog *DrHoxd9a* has a Foxp1 MD in proximity to the RD (see also A) and induced ectopic PGC (*Bmp5*⁺) neurons at brachial levels.

(H) Amphioxus Hox9 induced ectopic LMC (Foxp1^{high}, *Raldh2*⁺) neurons at thoracic levels.

(I) *DrHoxd9a*NΔ140 lacking both Hox RD and Foxp1 MD failed to suppress Foxp1, and induced ectopic LMC neurons at thoracic levels.

(J and K) Internal deletion of the RD region [*MmHoxc9*NΔ(73–101)] or MD [*MmHoxc9*NΔ(114–121)] failed to unmask LMC-promoting activity.

(L) LMC neurons were induced by *MmHoxc9*NΔ(73–121), which lacks both the RD and MD.

See also Figure S5.

consistent with the idea that the sites are required for Hoxc9-mediated exclusion of *Foxp1* from this population (Figure 7E; Figure S7D). These results indicate that the Hox sites are essential for the regulation of *Foxp1* in MNs.

Competitive Hox Interactions at the *Foxp1* Locus

Our findings suggest that Hoxc9 suppresses LMC identity through blocking the ability of Hox proteins to initiate *Foxp1* autoregulation. In principle, Hoxc9 could accomplish this by neutralizing the activity of LMC-promoting Hox proteins via interactions off DNA, or by competing at shared target sites within the *Foxp1* locus. To address these possibilities, we first tested whether Hoxc9 DNA binding is necessary for its repressive actions. We introduced mutations in highly conserved DNA recognition sequences of the Hoxc9 homeodomain (Gln50 → Ala and Asn51 → Ala), which diminish DNA binding but preserve homeo-domain structure (Remacle et al., 2002). Expression of this construct at brachial levels had no effect on *Foxp1* or anterior *Hox* genes, indicating that DNA binding is required for Hoxc9 activities (Figure 7F). We also used gel mobility shift assays to test whether Hoxc9 can displace Hoxc6 from sites in the *Foxp1* gene. This analysis revealed that Hoxc9 was effective in competing with Hoxc6 at sites in the *Foxp1* gene (Figure 7G). These data indicate that Hoxc9 requires DNA binding to repress LMC fate, and that Hoxc9 is capable of excluding LMC-promoting Hox proteins from *Foxp1*.

We next tested whether Hoxc9 acts by blocking maintenance of *Foxp1* expression. Ectopic expression of Hoxc9 at brachial levels inhibits LMC specification (Dasen et al., 2008); however, interpretation of this finding is confounded by the repressive effects of Hoxc9 on brachial *Hox* genes. To circumvent this issue, we coexpressed Hoxc6 and Hoxc9 at brachial levels, reasoning that if MNs were confronted with both Hoxc9 and Hoxc6, Hoxc9 would suppress *Foxp1* autoregulation and favor PGC specification, independent of its repressive actions toward *Hox* genes. We optimized conditions so that the expression levels of each construct were similar to levels normally found in MNs (Figure S7F). MNs coexpressing Hoxc6 and Hoxc9 at brachial levels expressed low *Foxp1* levels and acquired a PGC identity, as assessed by *Bmp5* induction (Figure 7H). In contrast, MNs expressing Hoxc6 alone or in combination with the LMC-inducing Hoxc9 mutant derivative retained an LMC identity (*Foxp1*^{high}, *Raldh2*⁺) (Figure 7H; Figure S7E). These results indicate that Hoxc9 is capable of blocking activation of high levels of *Foxp1*, independent of its repressive activity toward *Hox* genes. Hoxc9 likely accomplishes this function in vivo by displacing Hox proteins that would otherwise promote LMC identity, many of which are expressed at low levels in thoracic segments (Jung et al., 2010; Lacombe et al., 2013). Thus, the organization of spinal motor columns relies on the sustained binding of Hoxc9 to the *Foxp1* locus, which acts to prevent LMC induction at thoracic levels.

DISCUSSION

Locomotion is a fundamental animal behavior, but the genetic programs that contributed to the emergence of limb-specific motor circuits are largely unexplored. In this study, we defined the mechanisms controlling the specification and organization

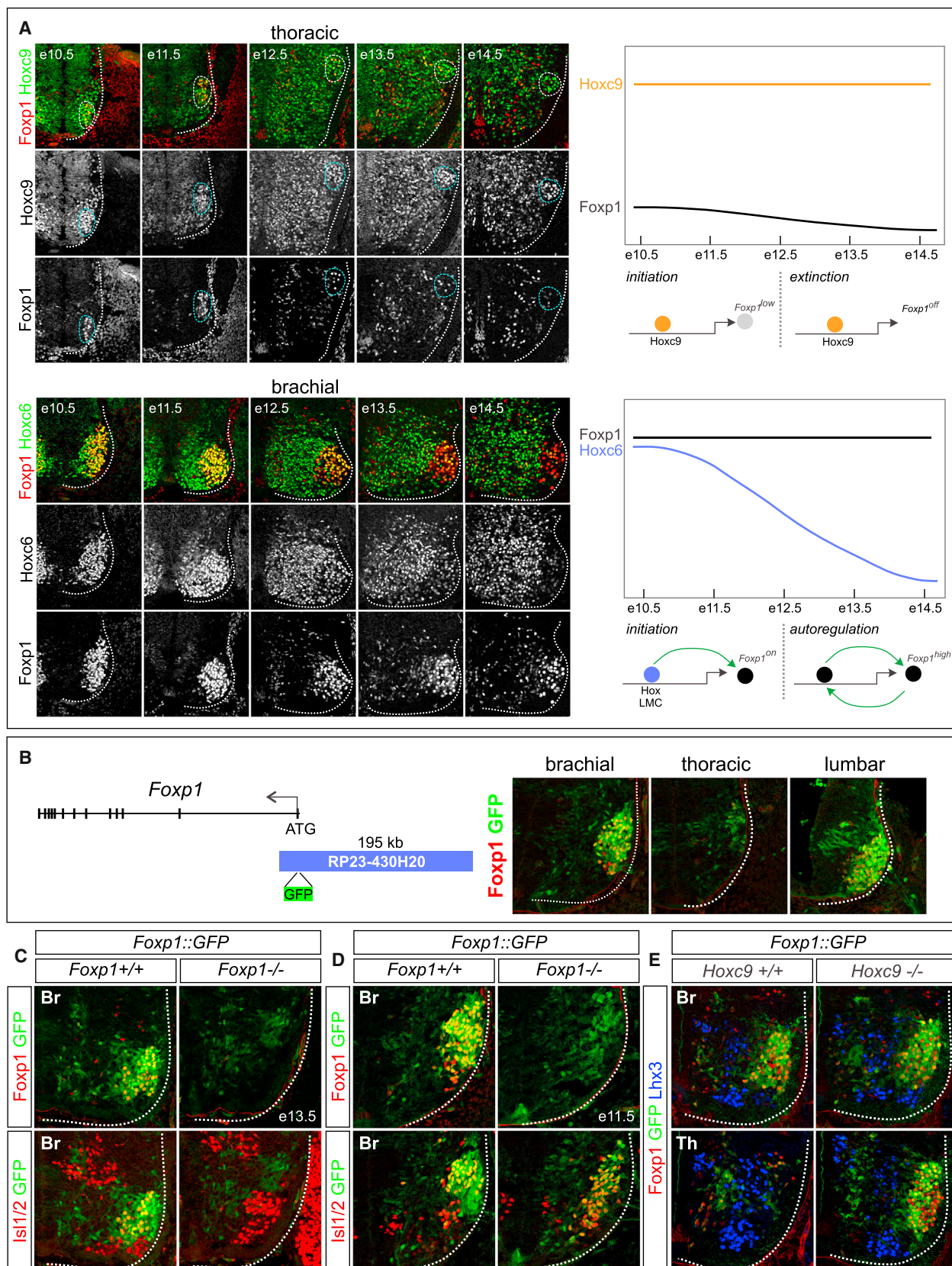
of MN subtypes required to coordinate limb muscles during ambulatory motor behaviors. We found that limb-innervating MNs are determined through a set of transient and permissive Hox inputs that initiate autoregulation of the *Foxp1* gene, and that the registry between LMC and limb position is defined by Hoxc9-mediated suppression of *Foxp1* at thoracic levels (Figure 8A). This specific activity is mediated through a modification in a subset of Hox9 proteins that appeared at the time vertebrates acquired paired appendages. Adjustment in the pattern of Hoxc9 expression in the neural tube likely contributes to the variety of columnar topographic arrangements among vertebrates. These studies thus offer insights into the strategies through which *Hox* genes facilitate evolution of the CNS.

Hox Activity Regulation and the Diversity of MN Columnar Organization

Hox genes are key determinants of morphological diversity across animal species (Burke et al., 1995; Carroll et al., 2005). In *Drosophila*, control of leg number is determined through a repressive motif in the Hox protein Ubx, which suppresses leg formation in abdominal segments (Galant and Carroll, 2002; Ronshaugen et al., 2002). Notably, this motif is absent from crustaceans that bear appendages in trunk segments. In vertebrates, the pattern of Hox activity in the lateral plate mesoderm determines the number and position of ribs (Vinagre et al., 2010). In snakes, mutation in a Hox-dependent *cis* element allows for rib formation in regions that would normally lack them (Guerreiro et al., 2013). Changes in the profiles of *Hox* expression are also correlated with the absence of limbs in snake embryos (Cohn and Tickle, 1999). Whether Hox proteins contribute to behavioral adaptations at the neural circuit level has not been addressed.

Our findings indicate that a key mechanism through which MN organization emerged involves modulation in Hox protein activities. We identified sequences within Hox9 proteins that confer differential effects on target gene regulation in vivo, and each motif appeared at a distinct phase of vertebrate evolution. All of the Hox9 proteins we tested possess a conserved N-terminal domain that can extinguish expression of brachial *Hox* genes in chick embryos. This repressive activity is present in the single Hox9 protein of amphioxus, suggesting a function at the base of the chordate lineage in establishing neuronal Hox profiles. In contrast, Hox9 proteins of appendage-bearing vertebrates display distinct activities in MNs, and only a subset suppress LMC fates. Repression of LMC identity by Hoxc9 is mediated by a distinct region that plays a more restricted role through differential effects on the *Foxp1* gene. The MD motif is active in the Hoxc9 protein of elephant shark, a representative of the most primitive appendage-bearing vertebrates, but is absent from the Hox9 protein of the limbless amphioxus. The presence of an MD or MD-like domain in three of the four mouse Hox9 paralogs suggests that this motif appeared prior to *Hox* cluster duplication events, implying that the first vertebrates bearing limb-like appendages may have contained a single *Hox* cluster.

At what stage during the evolution of limb-innervation programs did this specific repressive activity of Hoxc9 arise? One model posits that basal fin-bearing vertebrates contained a single fin extending the length of the trunk (Freitas et al., 2006; Tanaka et al., 2002; Tanaka and Onimaru, 2012). Subsequently, this elongate appendage was restricted to a rostral position,



giving rise to the pectoral fins. One could imagine a scenario where primitive fin-bearing vertebrates contained an LMC-like population extending the length of the spinal cord, and its confinement to pectoral and pelvic levels was coordinated with changes in fin position. Conceivably, this could have been achieved through the appearance of a new repressive motif in Hoxc9. Thus, we favor a model in which, at the time vertebrates acquired paired appendages, a new activity emerged that allowed a subset of *Hox9* genes to repress *Foxp1* and/or other genes that promote fin innervation (Figure 8B). This hypothesis does not exclude alternative origins of the pectoral fin, such as the gill arch (Gillis et al., 2009), which would have also necessitated a strategy for ensuring restriction of LMC-like populations.

CNS Organization as a Function of Modulation in *Hox* Expression Profiles

Our findings suggest that a key mechanism governing variations in MN organization is mediated by alterations in *Hox* profiles. We found that in snake embryos the domain of Hoxc9 expression is extended along the rostrocaudal axis and likely contributes to the absence of brachial LMC neurons. In contrast, species with relatively large appendages, such as the pectoral fins of stingrays and skates, could generate a broader distribution of LMC-like MN populations by attenuating the repressive influence of Hoxc9. Fin-innervating MN populations in stingrays extend ~80 segments (Coggeshall et al., 1978; Droege and Leonard, 1983), and it is tempting to speculate that this organization is mediated through regulation of column-defining *Hox* genes. Certain skate species lack the *HoxC* cluster in its entirety (King et al., 2011), and removal of the *Hoxc9* gene in this context could contribute to the extension of pectoral fin-innervating populations. Modification in the expression pattern of *Hoxc9* would, in principle, allow for efficient reorganization of MN populations in registry with changes in the appendicular musculoskeletal system (Figure 8C).

There are also significant differences in the mechanisms of *Hox* gene regulation at limb and thoracic levels. At limb levels, *Hox* determinants are only transiently expressed by LMC neurons, and identity is preserved through *Foxp1* autoregulation. In contrast, *Foxp1* is transiently expressed by thoracic PGC neurons, whereas *Hoxc9* is maintained throughout early embryogenesis. *Hoxc9* is also distinct among *Hox* genes expressed by spinal MNs, as its function is required in MN progenitors and is highly susceptible to alterations in the activities of early determinants that control *Hox* expression, including morphogens and Polycomb group proteins (Dasen et al., 2003; Golden and Dasen, 2012). The multiple pathways through which the

Hoxc9 gene is regulated could serve to provide alternative strategies to modulate its spatial and temporal profile during adaptive changes in the CNS.

Hox genes are widely expressed in the nervous system (Philippidou and Dasen, 2013), and alterations in *Hox* activity profiles likely impact specification in multiple cell lineages, including the diverse interneuron populations that coordinate limb movement (Andersson et al., 2012; Lanuza et al., 2004). These ensembles of rhythmically active neurons are known to occupy specific rostrocaudal positions of the spinal cord (Ballion et al., 2001; Kjaerulff and Kiehn, 1996), and it is plausible that their connectivity is shaped by the same *Hox* networks that determine MN subtype identities. *Hox*-dependent programs could therefore exert a broader role in the evolution of motor circuits that foster behavioral adaptations.

EXPERIMENTAL PROCEDURES

Mouse Genetics

HoxC cluster (Suemori and Noguchi, 2000), *HoxA* cluster (Kmita et al., 2005), *Foxp1* (Wang et al., 2004), and *Hoxc9* (McIntyre et al., 2007) mutant strains have been previously described. BAC transgenic mice were generated by pronuclear microinjection using standard procedures. Procedures performed in this study involving animals were conducted in compliance with protocols approved by the Institutional Animal Care and Use Committee of the New York University School of Medicine.

Generation of BAC Transgenic Mice

The *Foxp1::GFP* reporter line was generated using BAC clone RP23-430H20 corresponding to chr6:99,097K–99,292K (mouse genome assembly mm9). Sequences flanking the *Foxp1* ATG were cloned into the shuttle vector pLD53SC-AEB and introduced into the BAC by homologous recombination (Gong et al., 2003). To generate *Foxp1::GFP-4c^{mut}*, a potential *Hox* binding site was mutated into an *Nsi*I site. A single region (3a) or both regions (3a and 4c) were deleted in the BAC to make *Foxp1::GFP-Δ3a* and *Foxp1::GFP-Δ3aΔ4c* transgenes, respectively. The genomic regions 3a and 4c were identified by *Hoxc9* chromatin immunoprecipitation sequencing (ChIP-seq) (Jung et al., 2010): region 3a, chr6:99,286,209–99,286,532; region 4c, chr6:99,140,045–99,140,206 (mm9).

In Ovo Chick Electroporations

Expression constructs for murine *Hox9* paralogs were generated as described previously (Dasen et al., 2003; Jung et al., 2010). Full-length zebrafish *Hoxc9a* and *Hoxd9a* cDNAs were obtained from Open Biosystems. To generate additional full-length *Hox9* cDNAs, exons were amplified by PCR from genomic DNA. In ovo electroporation was performed in Hamburger Hamilton (HH) stage 13–15 and analyzed at HH stage 27. In each electroporation, the expression plasmid (pCAGGs) was used in the range of 50–200 ng/μl with pBKS as carrier DNA (1 μg/μl). We titrated the amount of HA-tagged m*Hoxc9* or m*Hoxd9* mutant derivatives before further analysis to ensure that their expression levels were similar to an HA-tagged wild-type m*Hoxc9* or m*Hoxd9*. Results for each

Figure 6. LMC Specification Relies on *Foxp1* Autoregulation

- (A) Temporal patterns of Hox proteins and *Foxp1* in LMC and PGC neurons. At thoracic levels, *Hoxc9* expression was sustained between e10.5 and e14.5, whereas *Foxp1* was undetectable by e14.5. PGC positions are outlined by dotted circles. *Hoxc6* was transiently expressed by LMC neurons, whereas *Foxp1* was maintained. Model depicting differential regulation of *Foxp1* in LMC and PGC neurons. Both LMC-promoting Hox proteins and *Hoxc9* are required for *Foxp1* induction at e10.5–e11.5. At later embryonic stages, *Foxp1* autoregulation maintains LMC identity, whereas *Hoxc9* suppresses *Foxp1*.
 - (B) Generation of a *Foxp1* reporter line using a BAC spanning ~195 kb upstream of the *Foxp1* start codon. Analysis of *Foxp1::GFP* transgenic mice showing GFP expression recapitulates both the spatial profile and relative *Foxp1* levels at e11.5.
 - (C–E) Analysis of *Foxp1::GFP* reporter mice in different mutant backgrounds.
 - (C) In *Foxp1* mutants, GFP was depleted from MNs (*Isl1/2⁺*) by e13.5, indicating a requirement for *Foxp1* protein to maintain its own expression.
 - (D) At e11.5, in *Foxp1* mutants, GFP expression was detected in MNs, indicating that initial activation is retained.
 - (E) In the absence of *Hoxc9*, GFP was expressed at high levels by ectopic LMC neurons at thoracic levels at e12.5.
- See also Figure S6.

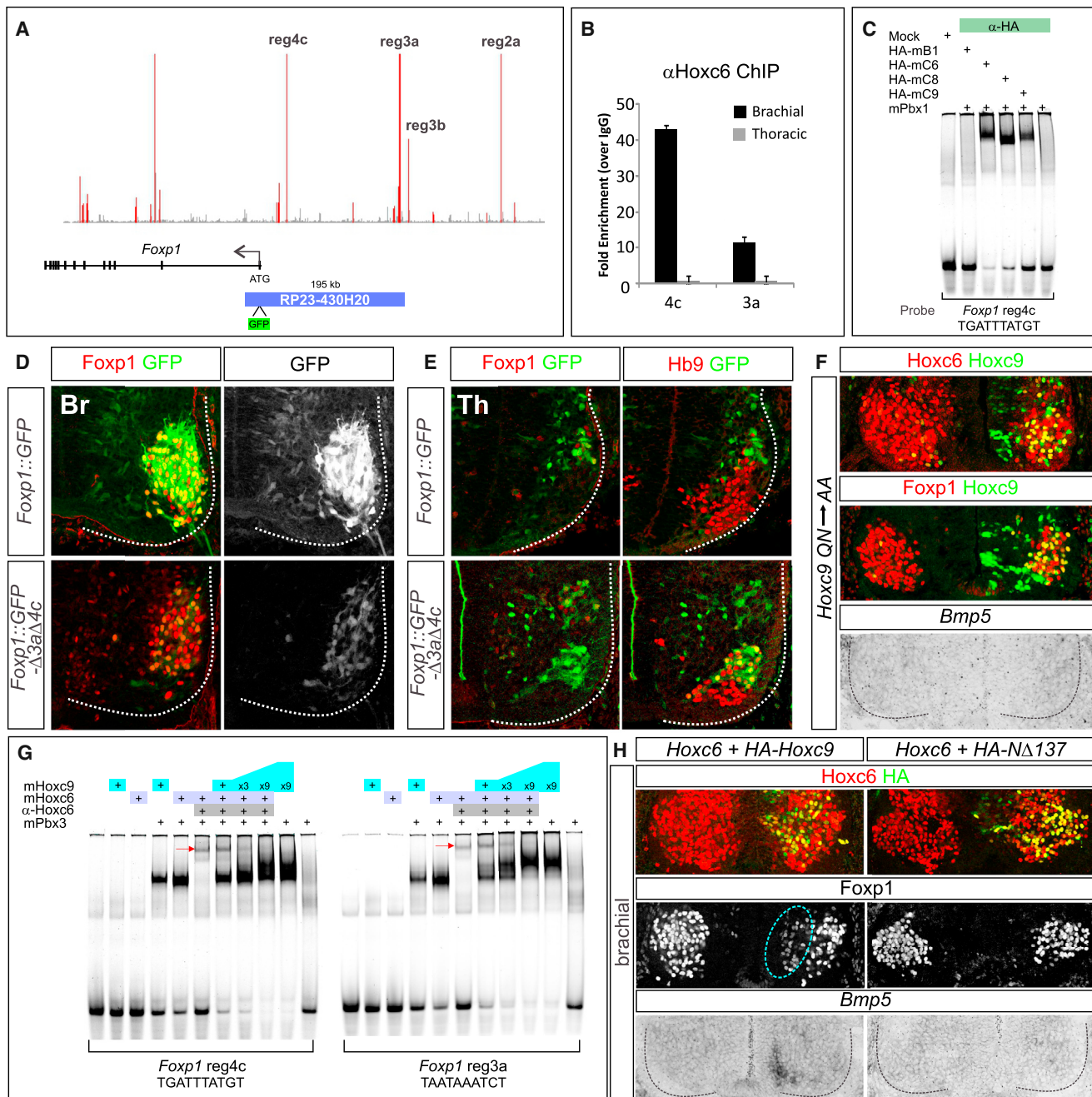


Figure 7. Hoxc9 Dominantly Suppresses LMC Specification

- (A) ChIP-seq signal map of Hoxc9 binding near the *Foxp1* locus in embryonic stem cell-derived MNs. Location of the BAC clone used for the *Foxp1* reporter is indicated.
 - (B) ChIP assays showing that Hoxc6 binds to *Foxp1* elements identified by Hoxc9 ChIP-seq. Error bars represent SEM on duplicates.
 - (C) Multiple Hox proteins including mHoxc6, mHoxc8, and mHoxc9 bound with mPbx1 to the *Foxp1* sites, whereas mHoxb1 failed to bind in vitro.
 - (D) and (E) Founder analysis of *Foxp1*::GFP- Δ 3a Δ 4c reporter lacking two Hox binding sites (see also Figure S7D).
 - (D) At brachial levels, the GFP reporter was dramatically reduced relative to *Foxp1*::GFP.
 - (E) At thoracic levels, ectopic GFP was detected in HMC neurons in *Foxp1*::GFP- Δ 3a Δ 4c embryos.
 - (F) Expression of the *Hoxc9*^{QN \rightarrow AA} DNA binding mutant at brachial levels failed to repress Hox genes or induce columnar identities.
 - (G) Competition assays for DNA binding. Hoxc9 can displace Hoxc6 from binding sites within the *Foxp1* gene. A Hoxc6 antibody was used to supershift the complex to distinguish it from Hoxc9 binding at the sites. The red arrows indicate a supershifted Hoxc6 complex.
 - (H) Coelectroporation showing that Hoxc9 dominantly suppressed LMC differentiation in the presence of Hoxc6, and induced ectopic PGC (*Bmp5*⁺) neurons at brachial levels (indicated by the dotted circle). Hoxc9 acts by displacing LMC-promoting Hox proteins from the *Foxp1* locus. When Hoxc6 was misexpressed with mHoxc9NΔ137, coelectroporated cells retained LMC identity.
- See also Figure S7.

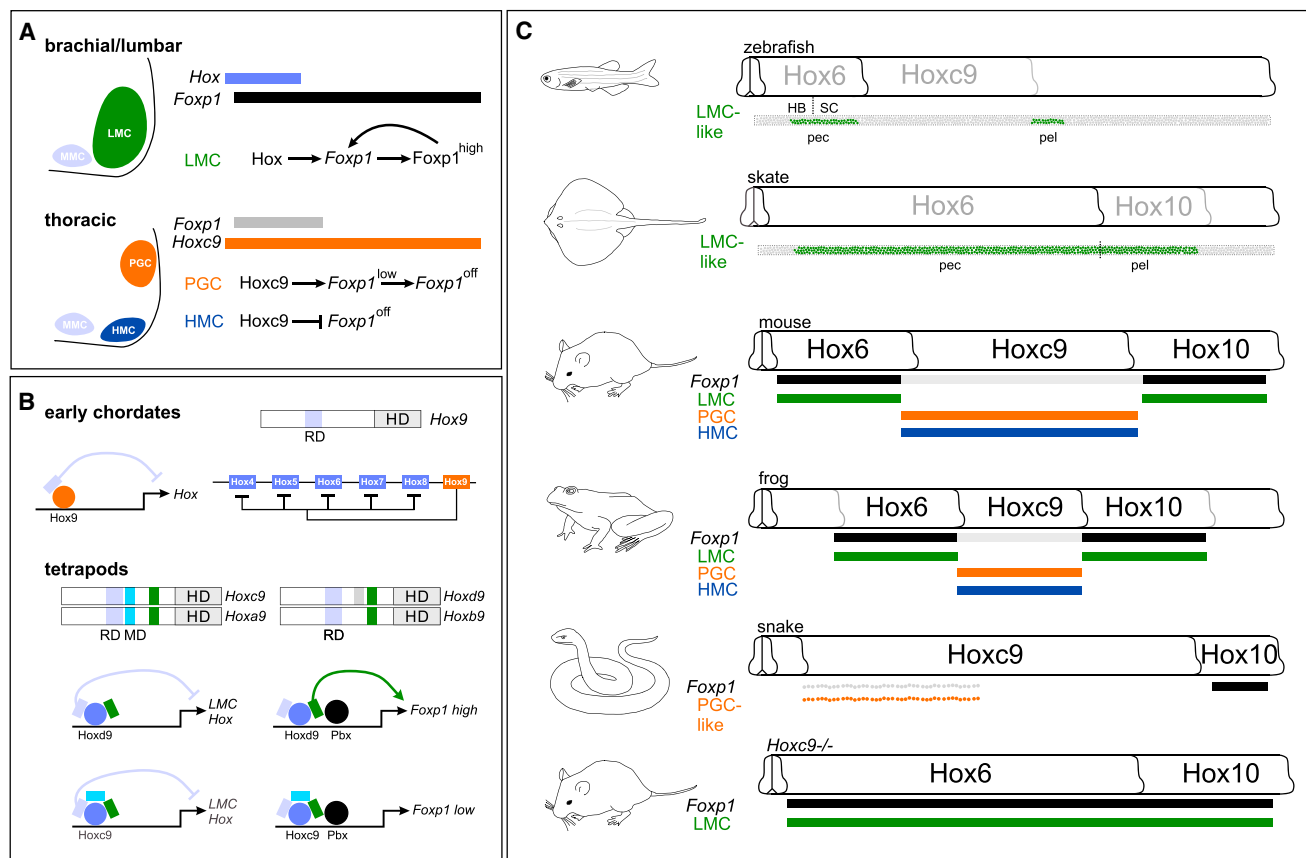


Figure 8. Model for the Evolution of Hox-Dependent Motor Columns

(A) Temporal regulation of *Foxp1* by Hox proteins during MN columnar specification. In LMC neurons, transient Hox activity initiates *Foxp1* autoregulation. At thoracic levels, Hoxc9 initiates low-level and transient *Foxp1* expression in PGC neurons and represses *Foxp1* in HMC neurons.

(B) Model for the evolution of functional domains within Hox9 proteins. A domain capable of repressing anterior *Hox* genes is present in Hox9 proteins of early chordates. A modulatory domain within tetrapod Hoxa9 and Hoxc9 appeared in appendage-bearing vertebrates and is required for suppression of LMC identity at thoracic levels.

(C) Speculative model for MN organization by evolving Hox activity profiles. MN columnar organization is controlled through species-specific Hox profiles to accommodate different vertebrate body plans. In zebrafish the posterior boundary of pectoral fin MNs (pec) corresponds to the anterior boundary of Hoxc9 expression (Ma et al., 2010). The hindbrain (HB)/spinal cord (SC) boundary is indicated. Skate is shown as a representative species having an extended pectoral fin that develops adjacent to the pelvic fin (pel), whereas frogs bear the fewest number of thoracic segments among land vertebrates. In both species the position and distribution of LMC-like MNs may be defined by the profile of Hoxc9 activity. The expanded profile of Hoxc9 in snakes suppresses LMC differentiation at rostral levels. In mice mutant for the *Hoxc9* gene, LMC neurons extend from cervical to lumbar levels.

experiment are representative of at least three embryos in which the electroporation efficiency in MNs was >60%.

ChIP Assays

Chromatin immunoprecipitation was performed as described previously (Jung et al., 2010) on e12.5–e13.5 mouse spinal cords using rabbit anti-Hoxc6 (Abcam; ab41587). Genomic regions were amplified using Power SYBR Green PCR Master Mix (Applied Biosystems) and detected with an Mx3005P real-time PCR apparatus (Stratagene). Fold enrichments were calculated over IgG using the $\Delta\Delta Ct$ method: fold enrichment = $2^{-(\Delta\Delta Ct)}$, where $\Delta\Delta Ct = (Ct_{IP} - Ct_{Input}) - (Ct_{IgG} - Ct_{Input})$. Primer sequences used for the real-time PCR were as follows: *Foxp1* reg3a_fw: 5'-GTCTCAAGGGAGGGAAAAA-3'; *Foxp1* reg3a_rev: 5'-GGGATAGTGGCGTTAAC-3'; *Foxp1* reg4c_fw: 5'-ATCGCTCCCACCCA TAAAG-3'; *Foxp1* reg4c_rev: 5'-ATCTCGGGTGTGAGAATGA-3'.

In Situ Hybridization and Immunohistochemistry

Fixed embryos were sectioned at 16 μ m by cryostat. *In situ* hybridization and immunohistochemistry were performed as described (Tsuchida et al., 1994). Antibodies against Hox proteins, LIM HD proteins, and other proteins were

generated or obtained as described (Dasen et al., 2005; Jung et al., 2010; Liu et al., 2001; Tsuchida et al., 1994). Additional antibodies used were monoclonal anti-HA (1:10,000; Covance) and goat polyclonal anti-GFP (1:4,000; Rockland).

Electrophoretic Mobility Shift Assays

Electrophoretic mobility shift assays were performed as described previously (Lacombe et al., 2013). 293T cells were transfected with expression constructs using Lipofectamine 2000 (Invitrogen), and nuclear extracts were prepared as described (Wadman et al., 1997). Protein amounts were estimated by western blot. For competition assays, recombinant proteins were prepared as described (Lacombe et al., 2013). Protein amounts in Figure 7G were as follows: mHoxc6, 4 pmol in lanes 3, 5, 6, 7, 8, and 9. mHoxc9, 4 pmol in lanes 2, 4, and 7; 12 pmol in lane 8; and 36 pmol in lanes 9 and 10. mPbx3, 4 pmol in lanes 4, 5, and 6; 8 pmol in lane 7; 16 pmol in lane 8; and 40 pmol in lanes 9, 10, and 11. The sense sequences for the probes were as follows: *Hoxc4* reg1, 5'-ATCCCGAGACTGATTATGACGTTTACAGCC-3'; *Foxp1* reg3a, 5'-ATGCCGACATAATAATCTAATCAAGTCTAC-3'; *Foxp1* reg4c, 5'-ATGTTGGAGGTCTGATTATGTTGTCATTCTC-3'. Hoxc9 binding sites

are underlined in each oligomer. Fifteen base pairs of linker sequence (CCTCGTCCCACAGCT) was added to each probe for the IRDye-800 labeling. Anti-HA antibody (0.5–1 µg) (Covance) and anti-Hoxc6 antibody (1 µg) (Abcam; ab41587) were used in supershifts.

Sequence Comparisons

Protein sequence alignments were generated using AlignX in Vector NTI (Invitrogen). The UCSC Genome Browser (<http://genome.ucsc.edu>) was used to compare vertebrate *Foxp1* sequences.

Quantification of Protein Levels

Nuclear *Foxp1*, *Hoxc6*, and *Hoxc9* levels were measured as described (Dasen et al., 2008). Mean pixel intensities for >100 MN nuclei are shown.

SUPPLEMENTAL INFORMATION

Supplemental Information includes seven figures and can be found with this article online at <http://dx.doi.org/10.1016/j.devcel.2014.03.008>.

ACKNOWLEDGMENTS

We thank Olivier Pourquie for generously providing snake and whiptail lizard embryos; Chris Amemiya for coelacanth and amphioxus BAC clones; Martin Cohn for lamprey sequences; Tarang K. Mehta for lamprey gDNA and *Hox9* sequences; and Claude Desplan, Gord Fishell, Hyung Don Ryoo, and laboratory members for providing valuable feedback. We thank the NYU Mouse Transgenic Facility for BAC transgenics; Julie Lacombe and Doug Epstein for assistance with recombineering; Shaun Mahony for analysis of ChIP-seq data; and Carolyn Walsh, Jonathan Grinstein, and David Lee for technical assistance. B.V. is supported by the Biomedical Research Council of A*STAR, Singapore. D.D. is supported by grants from the Swiss National Research Foundation and the European Research Council. J.S.D. is supported by funding from the Howard Hughes Medical Institute and the National Institutes of Health (R01 NS062822).

Received: January 27, 2014

Revised: March 7, 2014

Accepted: March 13, 2014

Published: April 17, 2014

REFERENCES

- Andersson, L.S., Larhammar, M., Memic, F., Wootz, H., Schwochow, D., Rubin, C.J., Patra, K., Arnason, T., Wellbring, L., Hjälm, G., et al. (2012). Mutations in DMRT3 affect locomotion in horses and spinal circuit function in mice. *Nature* 488, 642–646.
- Ballion, B., Morin, D., and Viala, D. (2001). Forelimb locomotor generators and quadrupedal locomotion in the neonatal rat. *Eur. J. Neurosci.* 14, 1727–1738.
- Begemann, G., Schilling, T.F., Rauch, G.J., Geisler, R., and Ingham, P.W. (2001). The zebrafish neckless mutation reveals a requirement for raldh2 in mesodermal signals that pattern the hindbrain. *Development* 128, 3081–3094.
- Burke, A.C., Nelson, C.E., Morgan, B.A., and Tabin, C. (1995). Hox genes and the evolution of vertebrate axial morphology. *Development* 121, 333–346.
- Carroll, S.B., Grenier, J.K., and Weatherbee, S.D. (2005). From DNA to Diversity: Molecular Genetics and the Evolution of Animal Design, Second Edition. (Malden, MA: Blackwell).
- Coggshall, R.E., Leonard, R.B., Applebaum, M.L., and Willis, W.D. (1978). Organization of peripheral nerves and spinal roots of the Atlantic stingray, *Dasyatis sabina*. *J. Neurophysiol.* 41, 97–107.
- Cohn, M.J., and Tickle, C. (1999). Developmental basis of limblessness and axial patterning in snakes. *Nature* 399, 474–479.
- Daeschler, E.B., Shubin, N.H., and Jenkins, F.A., Jr. (2006). A Devonian tetrapod-like fish and the evolution of the tetrapod body plan. *Nature* 440, 757–763.
- Dasen, J.S., and Jessell, T.M. (2009). Hox networks and the origins of motor neuron diversity. *Curr. Top. Dev. Biol.* 88, 169–200.
- Dasen, J.S., Liu, J.P., and Jessell, T.M. (2003). Motor neuron columnar fate imposed by sequential phases of Hox-c activity. *Nature* 425, 926–933.
- Dasen, J.S., Tice, B.C., Brenner-Morton, S., and Jessell, T.M. (2005). A Hox regulatory network establishes motor neuron pool identity and target-muscle connectivity. *Cell* 123, 477–491.
- Dasen, J.S., De Camilli, A., Wang, B., Tucker, P.W., and Jessell, T.M. (2008). Hox repertoires for motor neuron diversity and connectivity gated by a single accessory factor, FoxP1. *Cell* 134, 304–316.
- Droge, M.H., and Leonard, R.B. (1983). Organization of spinal motor nuclei in the stingray, *Dasyatis sabina*. *Brain Res.* 276, 201–211.
- Fetcho, J.R. (1992). The spinal motor system in early vertebrates and some of its evolutionary changes. *Brain Behav. Evol.* 40, 82–97.
- Freitas, R., Zhang, G., and Cohn, M.J. (2006). Evidence that mechanisms of fin development evolved in the midline of early vertebrates. *Nature* 442, 1033–1037.
- Galant, R., and Carroll, S.B. (2002). Evolution of a transcriptional repression domain in an insect Hox protein. *Nature* 415, 910–913.
- Gillis, J.A., Dahn, R.D., and Shubin, N.H. (2009). Shared developmental mechanisms pattern the vertebrate gill arch and paired fin skeletons. *Proc. Natl. Acad. Sci. USA* 106, 5720–5724.
- Golden, M.G., and Dasen, J.S. (2012). Polycomb repressive complex 1 activities determine the columnar organization of motor neurons. *Genes Dev.* 26, 2236–2250.
- Gong, S., Zheng, C., Doughty, M.L., Losos, K., Didkovsky, N., Schambra, U.B., Nowak, N.J., Joyner, A., Leblanc, G., Hatten, M.E., and Heintz, N. (2003). A gene expression atlas of the central nervous system based on bacterial artificial chromosomes. *Nature* 425, 917–925.
- Grillner, S., and Jessell, T.M. (2009). Measured motion: searching for simplicity in spinal locomotor networks. *Curr. Opin. Neurobiol.* 19, 572–586.
- Guerreiro, I., Nunes, A., Woltering, J.M., Casaca, A., Nôvoa, A., Vinagre, T., Hunter, M.E., Duboule, D., and Mallo, M. (2013). Role of a polymorphism in a Hox/Pax-responsive enhancer in the evolution of the vertebrate spine. *Proc. Natl. Acad. Sci. USA* 110, 10682–10686.
- Izpísúa-Belmonte, J.C., Falkenstein, H., Dollé, P., Renucci, A., and Duboule, D. (1991). Murine genes related to the *Drosophila* AbdB homeotic genes are sequentially expressed during development of the posterior part of the body. *EMBO J.* 10, 2279–2289.
- Jung, H., Lacombe, J., Mazzoni, E.O., Liem, K.F., Jr., Grinstein, J., Mahony, S., Mukhopadhyay, D., Gifford, D.K., Young, R.A., Anderson, K.V., et al. (2010). Global control of motor neuron topography mediated by the repressive actions of a single *hox* gene. *Neuron* 67, 781–796.
- Kawano, S.M., and Blob, R.W. (2013). Propulsive forces of mudskipper fins and salamander limbs during terrestrial locomotion: implications for the invasion of land. *Integr. Comp. Biol.* 53, 283–294.
- King, B.L., Gillis, J.A., Carlisle, H.R., and Dahn, R.D. (2011). A natural deletion of the HoxC cluster in elasmobranch fishes. *Science* 334, 1517.
- Kjaerulff, O., and Kiehn, O. (1996). Distribution of networks generating and coordinating locomotor activity in the neonatal rat spinal cord in vitro: a lesion study. *J. Neurosci.* 16, 5777–5794.
- Kmita, M., Tarchini, B., Zákány, J., Logan, M., Tabin, C.J., and Duboule, D. (2005). Early developmental arrest of mammalian limbs lacking HoxA/HoxD gene function. *Nature* 435, 1113–1116.
- Lacombe, J., Hanley, O., Jung, H., Philippidou, P., Surmeli, G., Grinstein, J., and Dasen, J.S. (2013). Genetic and functional modularity of Hox activities in the specification of limb-innervating motor neurons. *PLoS Genet.* 9, e1003184.
- Landmesser, L.T. (2001). The acquisition of motoneuron subtype identity and motor circuit formation. *Int. J. Dev. Neurosci.* 19, 175–182.
- Lanuza, G.M., Gosgnach, S., Pierani, A., Jessell, T.M., and Goulding, M. (2004). Genetic identification of spinal interneurons that coordinate left-right locomotor activity necessary for walking movements. *Neuron* 42, 375–386.
- Liu, J.P., Laufer, E., and Jessell, T.M. (2001). Assigning the positional identity of spinal motor neurons: rostrocaudal patterning of Hox-c expression by FGFs, Gdf11, and retinoids. *Neuron* 32, 997–1012.

- Ma, L.H., Gilland, E., Bass, A.H., and Baker, R. (2010). Ancestry of motor innervation to pectoral fin and forelimb. *Nat. Commun.* 1, 49.
- McIntyre, D.C., Rakshit, S., Yallowitz, A.R., Loken, L., Jeannotte, L., Capecchi, M.R., and Wellik, D.M. (2007). Hox patterning of the vertebrate rib cage. *Development* 134, 2981–2989.
- Murakami, Y., and Tanaka, M. (2011). Evolution of motor innervation to vertebrate fins and limbs. *Dev. Biol.* 355, 164–172.
- Philippidou, P., and Dasen, J.S. (2013). Hox genes: choreographers in neural development, architects of circuit organization. *Neuron* 80, 12–34.
- Remacle, S., Shaw-Jackson, C., Matis, C., Lampe, X., Picard, J., and Rezsöhazy, R. (2002). Changing homeodomain residues 2 and 3 of Hoxa1 alters its activity in a cell-type and enhancer dependent manner. *Nucleic Acids Res.* 30, 2663–2668.
- Ronshagen, M., McGinnis, N., and McGinnis, W. (2002). Hox protein mutation and macroevolution of the insect body plan. *Nature* 415, 914–917.
- Roussou, D.L., Gaber, Z.B., Wellik, D., Morrisey, E.E., and Novitch, B.G. (2008). Coordinated actions of the forkhead protein Foxp1 and Hox proteins in the columnar organization of spinal motor neurons. *Neuron* 59, 226–240.
- Shah, V., Drill, E., and Lance-Jones, C. (2004). Ectopic expression of Hoxd10 in thoracic spinal segments induces motoneurons with a lumbosacral molecular profile and axon projections to the limb. *Dev. Dyn.* 231, 43–56.
- Sockanathan, S., and Jessell, T.M. (1998). Motor neuron-derived retinoid signaling specifies the subtype identity of spinal motor neurons. *Cell* 94, 503–514.
- Studer, M., Lumsden, A., Ariza-McNaughton, L., Bradley, A., and Krumlauf, R. (1996). Altered segmental identity and abnormal migration of motor neurons in mice lacking Hoxb-1. *Nature* 384, 630–634.
- Suemori, H., and Noguchi, S. (2000). Hox C cluster genes are dispensable for overall body plan of mouse embryonic development. *Dev. Biol.* 220, 333–342.
- Tanaka, M., and Onimaru, K. (2012). Acquisition of the paired fins: a view from the sequential evolution of the lateral plate mesoderm. *Evol. Dev.* 14, 412–420.
- Tanaka, M., Münsterberg, A., Anderson, W.G., Prescott, A.R., Hazon, N., and Tickle, C. (2002). Fin development in a cartilaginous fish and the origin of vertebrate limbs. *Nature* 416, 527–531.
- Thor, S., and Thomas, J.B. (2002). Motor neuron specification in worms, flies and mice: conserved and ‘lost’ mechanisms. *Curr. Opin. Genet. Dev.* 12, 558–564.
- Tripodi, M., and Arber, S. (2012). Regulation of motor circuit assembly by spatial and temporal mechanisms. *Curr. Opin. Neurobiol.* 22, 615–623.
- Tsuchida, T., Ensini, M., Morton, S.B., Baldassare, M., Edlund, T., Jessell, T.M., and Pfaff, S.L. (1994). Topographic organization of embryonic motor neurons defined by expression of LIM homeobox genes. *Cell* 79, 957–970.
- Vermot, J., Schuhbaur, B., Le Mouellic, H., McCaffery, P., Garnier, J.M., Hentsch, D., Brûlet, P., Niederreither, K., Chambon, P., Dollé, P., and Le Roux, I. (2005). Retinaldehyde dehydrogenase 2 and Hoxc8 are required in the murine brachial spinal cord for the specification of Lim1+ motoneurons and the correct distribution of Islet1+ motoneurons. *Development* 132, 1611–1621.
- Vinagre, T., Moncaut, N., Carapuço, M., Nóvoa, A., Bom, J., and Mallo, M. (2010). Evidence for a myotomal Hox/Myf cascade governing nonautonomous control of rib specification within global vertebral domains. *Dev. Cell* 18, 655–661.
- Wadman, I.A., Osada, H., Grütz, G.G., Agulnick, A.D., Westphal, H., Forster, A., and Rabbitts, T.H. (1997). The LIM-only protein Lmo2 is a bridging molecule assembling an erythroid, DNA-binding complex which includes the TAL1, E47, GATA-1 and Ldb1/NLI proteins. *EMBO J.* 16, 3145–3157.
- Wang, B., Weidenfeld, J., Lu, M.M., Maika, S., Kuziel, W.A., Morrisey, E.E., and Tucker, P.W. (2004). Foxp1 regulates cardiac outflow tract, endocardial cushion morphogenesis and myocyte proliferation and maturation. *Development* 131, 4477–4487.
- Wu, Y., Wang, G., Scott, S.A., and Capecchi, M.R. (2008). Hoxc10 and Hoxd10 regulate mouse columnar, divisional and motor pool identity of lumbar motoneurons. *Development* 135, 171–182.